Energy-Efficient UAV Trajectory Plan for 6G Networks

Peng Qin[1,2(✉)], Xue Wu[1,2], Xiongwen Zhao[1,2], and Honghao Zhao[1,2]

[1] State Key Laboratory of Alternate Electrical Power System with Renewable Energy Sources, School of Electrical and Electronic Engineering, North China Electric Power University, Beijing 102206, China
qinpeng@ncepu.edu.cn

[2] Hebei Key Laboratory of Power Internet of Things Technology, North China Electric Power University, Baoding 071003, China

Abstract. Leveraging UAVs for access and Altitude Platform Stations (HAPSs) for data backhaul to construct the Air-Ground Integrated Network (AGIN) is a feasible solution to achieve seamless network coverage for remote IoT devices in future 6G era. However, the limited battery of IoT terminals and constrained onboard energy storage of UAVs make system energy-efficiency becomes a new concern. To cope with the challenge, we propose a C-NOMA AGIN model for remote area. Then, we investigate the UAV trajectory plan problem for maximizing system energy efficiency (EE). We provide the solution to obtain the near-optimal UAV trajectory and flight speed. Results prove that the proposed approach is superior to others in terms of EE.

Keywords: Trajectory plan · Air-ground integrated 6G network (AGIN 6G) · NOMA · Energy Efficiency (EE)

1 Introduction

Although the fifth generation (5G) mobile communication can meet the demand of Internet of Things (IoT) applications in hot spots, there is still urgent need for more economical and efficient network coverage in remote districts. Meanwhile, to build the space-air-ground integrated network (SAGIN) is proposed in the vision of the sixth generation (6G) mobile communication, which can achieve seamless network coverage and ubiquitous terminal access [1].

This work was supported in part by the National Natural Science Foundation of China under Grant 62201212, the Natural Science Foundation of Hebei Province under Grant F2022502017, the Zhejiang Key Laboratory of Medical Electronics and Digital Health under Grant MEDH202215, the State Key Laboratory of Alternate Electrical Power System with Renewable Energy Sources under Grant LAPS21018, the Fundamental Research Funds for the Central Universities under Grant 2021MS002, and the National Key Research and Development Program of China under Grant 2020YFB1806000.

Q. Liang et al. (Eds.): CSPS 2022, LNEE 873, pp. 143–151, 2023.
https://doi.org/10.1007/978-981-99-1260-5_18

The SAGIN usually consists of the space-based segment, the air-based segment and the ground segment [2]. Air-based unmanned aerial vehicle (UAV) network has more advantages, such as lower constructive cost, higher line-of-sight (LoS) capability and flexible deployment characteristics, which can supply access for IoT terminals in remote districts, high altitude platform station (HAPS) ensures much wider coverage [3]. Paper [4] proposed the UAV-assisted SAGIN model, which mainly analyzed the performance of UAV-assisted network, and through network optimization, the throughput and spectral efficiency of the system were improved. It can be seen that heterogeneous AGIN has become an effective scheme to solve the network coverage problem and improve the system performance, which provides an important reference for the study of this paper.

Related studies had been carried out on NOMA technology [5, 6]. Since traditional orthogonal multiple access (OMA)-based technology is no longer adequate, non-OMA (NOMA) that can recover information using successive interference cancellation (SIC) at the receiving end and achieve better spectrum efficiency, has become the focus [7]. Paper [5] proposed a NOMA technology combined with orthogonal frequency division multiplexing (OFDM) technology, which reduced the bit error rate and improved the system performance based on cyclic stationary equalization technology. However, as the increasing of users' number, the complexity of SIC greatly increases. Therefore, by dividing terminals into multiple clusters, clustered-NOMA (C-NOMA) is an effective solution to both improve system throughput while balancing spectrum efficiency and terminal complexity.

In heterogeneous networks, it is a significant concern to plan UAV trajectory to enhance the system performance considering the constrained on-board energy storage of UAV [8, 9, 10]. Paper [9] proposed an integrated air-ground network system supporting XAPS, which maximized the uplink reachable rate of the system through spectrum, power and position optimization of UAVs based on matching theory. Paper [10] proposed a UAV-assisted space-ground remote IoT network architecture, optimized the deployment of UAVs through successive convex approximation (SCA) method, and solved the energy-saving communication problem between UAVs and ground terminals. The above

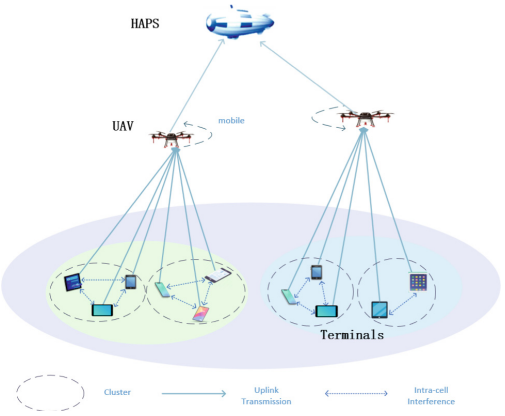

Fig. 1. C-NOMA-enabled AGIN 6G system model.

work mostly only considered communication energy consumption, however less likely to involve flight energy consumption, which have a greater effect on the capabilities of the UAV communication. So considering the flight trajectory and speed control, the propulsion energy consumption model of UAV is introduced to solve the optimization problem of trajectory and velocity of UAV, and achieve high EE and wide coverage of the system.

To cope with the above challenges for future remote IoT applications, we first put forward a C-NOMA AGIN model in this paper, including three segments of UAVs for massive access, HAPS for backhaul, and remote ground terminals. C-NOMA technology has stronger processing power and can achieve a balance between spectrum efficiency and complexity. Then, considering the finite battery of IoT terminals and limited energy storage on UAVs [11-13], we investigate the trajectory plan problem for maximizing system energy efficiency (EE). Solution is provided according to SCA and we obtain the near-optimal UAV trajectory. Simulations demonstrate that our approach is superior to others in terms of EE.

2 System Model

As shown in Fig. 1, we propose the C-NOMA-enabled AGIN 6G system model, including $\mathcal{U} = \{U_1, U_2, \ldots, U_M\}$ UAVs with flight altitude $\hat{h}_m$ for access, which share a channel with bandwidth of W, one HAPS with altitude H_A for backhaul, and $\mathcal{D} = \{D_1, D_2, \ldots, D_N\}$ terminal devices sharing a channel with bandwidth of W. The frequency resource is evenly divided into M blocks so that each UAV occupies different resource block without interference, and each block is further divided into $\mathcal{K} = \{S_1, S_2, \ldots, S_K\}$ subchannels. UAV serves its associated IoT devices using C-NOMA technology by dividing terminals into clusters. The flight period involves $\mathcal{T} = \{T_1, T_2, \ldots, T_L\}$ time slots, each of which is ΔT, and UAV flies back to the starting point when each cycle ends. Let $\mathbf{q}_m(t) = (x_m(t), y_m(t))$, $\mathbf{v}_m(t) \triangleq \dot{\mathbf{q}}_m(t)$, and $\mathbf{ac}_m(\mathrm{t}) \triangleq \ddot{\mathbf{q}}_m(t)$ respectively denote the location, speed and acceleration of the m th UAV in slot t. The position of the n th terminal is represented by $\mathbf{D}_n = (x_n, y_n, 0)$. Communication between terminal and UAV, UAV and HAPS is dominated by LoS links, and channel fading follows Rice fading [4, 10].

2.1 Communication Model

The distance between UAV m and user n in slot t is.

$$d_{n,m}(t) = \sqrt{\hat{h}_m^{\,2} + \|\mathbf{q}_m(t) - \mathbf{D}_n\|^2}, \forall n \in \mathcal{D}, m \in \mathcal{U}, t \in \mathcal{T}. \tag{1}$$

Then, the channel power gain occupying the k th subchannel can be expressed as.

$$h_{n,m,k}(t) = \frac{G_m G_n \beta_0}{d_{n,m}^2(t)}, \forall n \in \mathcal{D}, m \in \mathcal{U}, k \in \mathcal{S}, t \in \mathcal{T}, \tag{2}$$

where G_m and G_n are the directional antenna gains of UAV and user, respectively. β_0 represents the channel power gain at the reference distance $d_0 = 1\mathrm{m}$. Since HAPS is far

from UAVs, the distance can be replaced by H_A. Therefore, the channel gain from UAV m to HAPS is calculated by.

$$h_m = \frac{G_m G_2 \beta_0}{{H_A}^2}, \forall m \in \mathcal{U}, \tag{3}$$

where G_2 is the directional antenna gain of HAPS.

Suppose that in the t th slot, the transmission power from the n th user to the m th UAV is $P_{n,m,k}(t) \in \mathbf{P}^{\mathrm{D}\to\mathrm{U}}$, and the transmission power from the m th UAV to the HAPS is $P_m(t) \in \mathbf{P}^{\mathrm{U}\to\mathrm{H}}$. UAV trajectory, velocity and acceleration are defined as $\mathbf{Q} = \{\mathbf{q}_m(t), \forall m \in \mathcal{U}, t \in \mathcal{T}\}$, $\mathbf{V} = \{\mathbf{v}_m(t), \forall m \in \mathcal{U}, t \in \mathcal{T}\}$, $\mathbf{AC} = \{\mathbf{ac}_m(\mathrm{t}), \forall m \in \mathcal{U}, t \in \mathcal{T}\}$, respectively. The channel selection indicator between terminal and UAV is $\mathbf{A} = \left\{a_{n,m,k}(t), \forall n \in \mathcal{D}, m \in \mathcal{U}, k \in \mathcal{K}, t \in \mathcal{T}\right\}$, i.e., if terminal n connects with UAV m through the k th subchannel in the t th time slot, $a_{n,m,k}(t) = 1$; otherwise $a_{n,m,k}(t)$=0.

Then, the SINR between UAV m and terminal n occupying the k th subchannel can be calculated by

$$\gamma_{n,m,k}(t) = \frac{P_{n,m,k}(t) h_{n,m,k}(t)}{I_{n,m,k}(t) + N_0}, \tag{4}$$

where N_0 represents the noise power, $I_{n,m,k}(t) = \sum_{j=n+1}^{N} a_{j,m,k}(t) P_{j,m,k}(t) h_{j,m,k}(t)$ represents interference from other users in the same channel. SIC technology can be used to decode signals from terminal devices occupying the same sub-channel.

Likewise, the SINR between UAV m and HAPS can be calculated by.

$$\gamma_m(t) = \frac{P_m(t) h_m}{N_0}. \tag{5}$$

In the t th time slot, the uplink rate of user n to HAPS can be denoted by.

$$R_{n,m,k}(t) = \frac{W}{MK} log_2\left(1 + \frac{\gamma_{n,m,k}(t)\gamma_m(t)}{1 + \gamma_{n,m,k}(t) + \gamma_m(t)}\right). \tag{6}$$

The system capacity can be expressed as.

$$R = \frac{W}{MK} \sum_{t=1}^{L} \sum_{k=1}^{K} \sum_{m=1}^{M} \sum_{\mathrm{n}=1}^{N} a_{n,m,k}(t) log_2\left(1 + \frac{\gamma_{n,m,k}(t)\gamma_m(t)}{1 + \gamma_{n,m,k}(t) + \gamma_m(t)}\right). \tag{7}$$

2.2 Power Consumption Model

UAV power consumption includes two parts. One is the power associated with communication, including radiation, signal processing, and power generated by other circuits. The other is propulsion power consumption to maintain flight and maneuverability [14]. Fixed-wing UAVs used in this paper normally have no sudden deceleration and do not require engine to generate reverse thrust for the forward movement. Therefore, propulsion power consumption is a function of trajectory $\mathbf{q}_m(t)$ denoted by

$$P = \sum_{t=1}^{L} (P_d(t) + P_k(t)), \tag{8}$$

where $P_d(t) = \sum_{m=1}^{M}\left(c_1\|\mathbf{v}_m(t)\|^3 + \frac{c_2}{\|\mathbf{v}_m(t)\|}\left(1+\frac{\|\mathbf{ac}_m(t)\|^2-\frac{\left(\mathbf{ac}_m^T(t)\mathbf{v}_m(t)\right)^2}{\|\mathbf{v}_m(t)\|^2}}{g^2}\right)\right)$ represents the power required for overcoming drag, g denotes gravity, $P_k(t) = \sum_{m=1}^{M}\Delta k_m/\Delta T$, and $\Delta k_m = \frac{1}{2}m_m^{'}\left(\|\mathbf{v}_m(L)\|^2 - \|\mathbf{v}_m(1)\|^2\right)$ denotes the kinetic energy of flight in a cycle. $m_m^{'}$ is quality of UAV m, and c_1, c_2 are two parameters related to the weight of aircraft, air density, etc.

Then, the system EE is denoted by

$$\lambda = \frac{R}{P} \tag{9}$$

3 Problem Formulation

The objective is to maximize the uplink system EE for remote IoT terminals in AGIN by designing UAV trajectory plan and speed control, formulated as

$$\mathbf{P}0: \max_{\mathbf{Q},\mathbf{V}} \lambda$$

$$C1: \sum_{m=1}^{M}\sum_{k=1}^{K} a_{n,m,k}(t)R_{n,m,k}(t) \geq R_{min}(t) \tag{10}$$

$$C2: \sum_{k=1}^{K}\sum_{m=1}^{M}\sum_{n=1}^{N} a_{n,m,k}(t)R_{n,m,k}(t) \leq R_{max}^{H}(t) \tag{11}$$

$$C3: V_{min} \leq \|\mathbf{v}_m(t)\| \leq V_{max} \tag{12}$$

$$C4: \|\mathbf{ac}_m(t)\| \leq ac_{max} \tag{13}$$

Constraint (10) guarantees the system QoS. (11) represents the capacity constraint of the system with R_{max}^{H}, which guarantees that the total data transmitted cannot exceed the system capacity. (12), (13) denotes the speed and acceleration constraint of UAV, respectively.

4 Algorithm Analysis

The UAV trajectory, velocity and acceleration are all continuous variables, making **P**0 difficult to be solved directly. Therefore, we propose the algorithm for solving it based on SCA. The algorithm starts from line 3 with iteration index w. Line 4–5 achieves the best trajectory $(\mathbf{q}_m^w(t))^*$, speed $(\mathbf{v}_m^w(t))^*$, and acceleration $(\mathbf{ac}_m^w(t))^*$ for the current loop. It continues until the increase of the objective value is below a threshold ε. Details are shown below.

The denominator's upper bound of the objective function λ obtained from (8), the lower bound of system EE is

$$\lambda \geq \lambda_{lb} = \frac{R}{\sum_{t=1}^{L}\sum_{m=1}^{M}\left(c_1\|\mathbf{v}_m(t)\|^3 + \frac{c_2}{\|\mathbf{v}_m(t)\|}\left(1+\frac{\|\mathbf{ac}_m(t)\|^2}{g^2}\right) + \Delta k_m/\Delta T\right)}. \quad (14)$$

We can obtain the sub-optimal result based on first-order and second-order Taylor expansion:

$$\mathbf{v}_m(t+1) = \mathbf{v}_m(t) + \mathbf{ac}_m(t)\Delta T \quad (15)$$

$$\mathbf{q}_m(t+1) = \mathbf{q}_m(t) + \mathbf{v}_m(t)\Delta T + \frac{1}{2}\mathbf{ac}_m(t)\Delta T^2. \quad (16)$$

Notice that constraints (10)–(12) are non-convex. Both numerator and denominator of **P**0 are non-convex making the objective function non-convex. Therefore, we introduce the relaxation variable $\{\tau_m(t)\}$ and restate **P**0 as

$$\mathbf{P}1: \underset{\mathbf{Q},\mathbf{V}}{max} \frac{R}{\sum_{t=1}^{L}\sum_{m=1}^{M}\left(c_1\|\mathbf{v}_m(t)\|^3 + \frac{c_2}{\tau_m(t)} + \frac{c_2\|\mathbf{ac}_m(t)\|^2}{g^2\tau_m(t)} + \Delta k_m/\Delta T\right)}$$

$$\text{s.t.} C1 - C4$$

$$C5: \tau_m(t) \geq V_{min} \quad (17)$$

$$C6: \|\mathbf{v}_m(t)\|^2 \geq \tau_m(t)^2. \quad (18)$$

By this reformulation, the denominator of the objective function is convex for $\{\mathbf{v}_m(t), \mathbf{ac}_m(t), \tau_m(t)\}$, but new non-convex constraint (18) is created. To solve this non-convex constraint, we apply a locally convex approximation. With regard to any local point $\mathbf{v}_m^r(t)$ obtained in the r th iteration, we have

$$\|\mathbf{v}_m(t)\|^2 \geq \|\mathbf{v}_m^r(t)\|^2 + 2(\mathbf{v}_m^r(t))^T(\mathbf{v}_m(t) - \mathbf{v}_m^r(t)) \triangleq \psi_{lb}(\mathbf{v}_m(t)). \quad (19)$$

Thus, we define new constraints,

$$\psi_{lb}(\mathbf{v}_m(t)) \geq {\tau_m}^2(t). \quad (20)$$

Then, for the sake of solving the non-concavity of the numerator, it is transformed into

$$R = \frac{W}{MK}\sum_{t=1}^{L}\sum_{k=1}^{K}\sum_{m=1}^{M}\sum_{n=1}^{N} a_{n,m,k}(t)\left(\widehat{\gamma}_{n,m,k}(t) - \widehat{\gamma}'_{n,m,k}(t)\right) \quad (21)$$

$$\widehat{\gamma}_{n,m,k}(t) = log_2\left(\Omega_{n,m,k}(t) + P_{n,m,k}(t)h_{n,m,k}(t)P_m(t)h_m + \Theta_m(t)\right) \quad (22)$$

$$\widehat{\gamma}'_{n,m,k}(t) = log_2\big(\Omega_{n,m,k}(t) + \Theta_m(t)\big) \tag{23}$$

where $\Theta_m(t) = N_0^2 + N_0 P_m(t) h_m$

$$\Omega_{n,m,k}(t) = N_0 \sum_{j=n+1}^{N} \rho_{j,m,k}(t) h_{n,m,k}(t) + N_0 P_{n,m,k}(t) h_{n,m,k}(t) \sum_{j=n+1}^{N} \rho_{j,m,k}(t) h_{j,m,k}(t).$$

By using SCA method, the nonconvex problem is transformed into convex optimization problem. Owing to the space limitation, the derivation details are not shown, and similar derivation can be found in [6]. Finally, the numerator is concave, the denominator is convex, and all constraints are convex, making **P**0 transformed into a standard convex problem. Thus, using CVX can solve this problem.

Algorithm EE maximum SCA-based UAV Trajectory optimization algorithm

1: **Input:** $(\mathbf{q}_m(t))^{\mathbf{0}}, \varepsilon, w$
2: **Output:** $\mathbf{Q}^*, \mathbf{V}^*$
3: **repeat**
4: settle problem (**P0**) by using CVX to obtain $(\mathbf{q}_m^w(t))^*, (\mathbf{v}_m^w(t))^*$.
5: **update** $\mathbf{q}_m^{w+1}(t) = (\mathbf{q}_m^w(t))^*, \mathbf{v}_m^{w+1}(t) = (\mathbf{v}_m^w(t))^*$.
6: **update** iteration index w=w+1
7: **until** $|(\lambda'_{lb})^w - (\lambda'_{lb})^{w-1}| < \varepsilon$.
8: **return** $\mathbf{Q}^*, \mathbf{V}^*$.

5 Simulation Results

In this section, we make a comparison between the proposed algorithm and random trajectory method (Random) and OMA method using MATLAB. We consider 3 UAVs and 20 terminals randomly distributed in an area of 200 m × 120 m, each NOMA cluster contains two terminals.

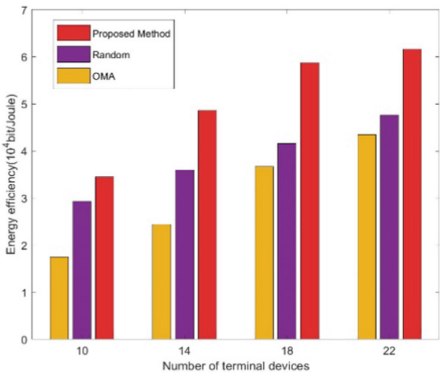

Fig. 2. The system EE for different benchmark algorithms.

Figure 2 shows the system EE for different benchmark algorithms. It is shown that as the number of users increases, so does energy efficiency. Moreover, compared with

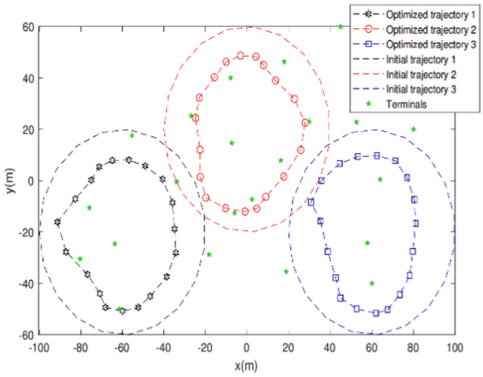

Fig. 3. Optimized trajectories for all UAVs.

OMA method and random trajectory method, our proposed method is always superior in terms of EE.

Figure 3 shows the optimized flight trajectories for three UAVs. It is shown that with the optimized trajectory, the UAV can get close to each terminal device as much as possible, so as to achieve better system EE and provide superior QoS.

6 Conclusion

In this paper, a C-NOMA-based heterogeneous AGIN network is proposed and we formulate the problem of maximizing the system EE by trajectory optimization. We design an algorithm to achieve the maximum system EE. Both theoretical analysis and results show that the proposed method is superior to others in terms of EE.

References

1. Li, B., Fei, Z., Zhang, Y.: UAV communications for 5G and beyond: recent advances and future trends. IEEE Internet Things J. **6**(2), 2241–2263 (2019)
2. Liu, J., Zhao, X., Qin, P., Geng, S., Meng, S.: Joint dynamic task offloading and resource scheduling for WPT enabled space-air-ground power internet of things. IEEE Trans. Network Sci. Eng. **9**(2), 660–677, March 2022
3. Qin, P., Fu, Y., Zhao, X., Wu, K., Liu, J., Wang, M.: Optimal task offloading and resource allocation for C-NOMA heterogeneous air-ground integrated power-IoT networks. IEEE Trans. Wireless Commun. (2022). https://doi.org/10.1109/TWC.2022.3175472
4. Wang, J., Jiang, C., Wei, Z., Pan, C., Zhang, H., Ren, Y.: Joint UAV hovering altitude and power control for space-air-ground IoT networks. IEEE Internet Things J. **6**(2), 1741–1753 (2019)
5. Datta, J., Lin, H.: Detection of uplink NOMA systems using joint SIC and cyclic FRESH filtering. In: 27th Wireless and Optical Communication Conference (WOCC), pp. 1–4 (2018)
6. Li, Y., Zhang, H., Long, K., Jiang, C., Gzuizani, M.: Joint resource allocation and trajectory optimization with QoS in UAV-based NOMA wireless networks. IEEE Trans. Wireless Commun. **20**(10), 6343–6355 (2021)

7. Kim, J., Kim, J., Park, S.: Joint design of power control and SIC decoding order for max-min fairness optimization in uplink NOMA systems. In: International Conference on Information Networking (ICOIN), pp. 339–342 (2021)
8. Qin, P., Zhu, Y., Zhao, X., Feng, X., Liu, J., Zhou, Z.: Joint 3D-location planning and resource allocation for XAPS-enabled C-NOMA in 6G heterogeneous internet of things. IEEE Trans. Veh. Technol. **70**(10), 10594–10609 (2021)
9. Zeng, Y., Zhang, R.: Energy-efficient UAV communication with trajectory optimization. IEEE Trans. Wirel. Commun. **16**(6), 3747–3760, June. 2017
10. Na, Z., Liu, Y., Shi, J., Liu, C., Gao, Z.: UAV-supported clustered NOMA for 6G-enabled internet of things: trajectory planning and resource allocation. IEEE Internet Things J. **8**(20), 15041–15048 (2021)
11. Qin, P., Fu, Y., Tang, G., Zhao, X., Geng, S.: Learning based energy efficient task offloading for vehicular collaborative edge computing. IEEE Trans. Veh. Technol. (2022). https://doi.org/10.1109/TVT.2022.3171344
12. Qin, P., Fu, Y., Feng, X., Zhao, X., Wang, S., Zhou, Z.: Energy efficient resource allocation for parked cars-based cellular-V2V heterogeneous networks. IEEE Internet Things J. **9**(4), 3046–3061 (2022)
13. Qin, P., Wang, M., Zhao, X., Geng, S.: Content service oriented resource allocation for space-air-ground integrated 6g networks: a three-sided cyclic matching approach. IEEE Internet Things J. (2022). https://doi.org/10.1109/JIOT.2022.3203793
14. Wu, X., Wei, Z., Cheng, Z., Zhang, X.: Joint optimization of UAV trajectory and user scheduling based on NOMA technology. In: IEEE Wireless Communications and Networking Conference (WCNC), pp. 1–6 (2020)